Partonic Effects on Pion Interferometry at the Relativistic Heavy Ion Collider

Zi-wei Lin, C.M. Ko, and Subrata Pal
Cyclotron Institute and Physics Department, Texas A&M University, College Station, Texas 77843-3366

Using a multiphase transport (AMPT) model that includes both initial partonic and final hadronic interactions, we study the pion interferometry at the Relativistic Heavy Ion Collider. We find that the two-pion correlation function is sensitive to the magnitude of the parton scattering cross section, which controls the parton density at which the transition from the partonic to hadronic matter occurs. Also, the emission source of pions is non-Gaussian, leading to source radii that can be more than twice larger than the radius parameters extracted from a Gaussian fit to the correlation function.

PACS numbers: 25.75.Gz, 24.10.Lx

Particle interferometry based on the Hanbury-Brown Twiss (HBT) effect has long been used to measure the size of an emission source [1]. In heavy ion collisions, it has been suggested that the HBT study can provide information not only on the spatial extent of the emission source but also on its expansion velocity and emission duration [2, 3, 4, 5]. In particular, the long emission time as a result of the phase transition from the quark-gluon plasma to hadronic matter in relativistic heavy ion collisions is expected to lead to an emission source which has a much larger radius in the direction of the total transverse momentum of detected two particles ($R_{\rm out}$) than that perpendicular to both this direction and the beam direction ($R_{\rm side}$) [5, 6, 7]. Since the quark-gluon plasma is expected to be formed in heavy ion collisions at the Relativistic Heavy Ion Collider (RHIC), it is thus surprising to find that the extracted ratio $R_{\rm out}/R_{\rm side}$ from a Gaussian fit to the measured two-pion correlation function in Au+Au collisions is close to one [8, 9, 10]. Also, the extracted radius parameters are small compared to theoretical predictions based on the hydrodynamical model [6]. These experimental results, especially the small value of $R_{\rm out}/R_{\rm side}$, have been attributed to strong space-time and momentum correlations in the emission source [11].

In this Letter, a multiphase transport model (AMPT) [12, 13, 14], that includes both initial partonic and final hadronic interactions, is used to study the pion interferometry in central Au+Au collisions at RHIC at $\sqrt{s} = 130A$ GeV. The AMPT model is a hybrid model that uses the minijet partons from hard processes and the strings from soft processes in the HIJING model [15] as the initial conditions for modeling the collision dynamics. The time evolution of partons is then modeled by the ZPC [16] parton cascade model. At present, this model includes only parton-parton elastic scatterings with an in-medium cross section given by:

$$\frac{d\sigma_p}{d\hat{t}} = \frac{9\pi\alpha_s^2}{2}\left(1+\frac{\mu^2}{\hat{s}}\right)\frac{1}{(\hat{t}-\mu^2)^2}, \qquad (1)$$

where the strong coupling constant α_s is taken to be 0.47, and $\hat{s}$ and $\hat{t}$ are the Mandelstam variables. The effective screening mass μ depends on the temperature and density of the partonic matter but is taken as a parameter for fixing the magnitude and angular distribution of the parton scattering cross section. After these minijet partons stop interacting, they are combined with their parent strings to fragment to hadrons using the Lund string fragmentation model as implemented in the PYTHIA routine [17]. The final-state hadronic scatterings are then modeled by the ART model [18].

The default AMPT model has been quite successful in describing the measured rapidity distributions of charge particles, particle to antiparticle ratios, and the spectra of low transverse momentum pions and kaons [13] in heavy ion collisions at the Super Proton Synchrotron (SPS) and RHIC. Since the initial energy density in Au+Au collisions at RHIC is expected to be much larger than the critical energy density at which the hadronic matter to quark-gluon plasma transition would occur [19, 20], the AMPT model has been extended to convert the initial excited strings into partons [14]. In this string melting scenario, hadrons, that would have been produced from string fragmentation, are converted instead to valence quarks and/or antiquarks. Interactions among these partons are again described by the ZPC parton cascade model. The transition of the partonic matter to the hadronic matter is, however, achieved using a simple coalescence model, which combines two nearest partons into mesons and three nearest partons into baryons or anti-baryons. Using parton scattering cross sections of 6-10 mb, the extended AMPT model is able to reproduce both the centrality and transverse momentum (below 2 GeV/c) dependence of the elliptic flow measured in Au+Au collisions at $\sqrt{s} = 130A$ GeV at RHIC [21].

From the AMPT model, the source of emitted particles is obtained from their space-time coordinate x and momentum $\mathbf{p}$ at freezeout, i.e., at their last interactions. Denoting the single-particle emission function for pions by $S(x,\mathbf{p})$, the HBT correlation function for two identical pions in the absence of final-state interactions, such as the Coulomb interaction, is then given by [2, 22]:

$$C_2(\mathbf{Q},\mathbf{K}) = 1 + \frac{\int d^4x_1 d^4x_2 S(x_1,\mathbf{K}) S(x_2,\mathbf{K}) \cos[Q\cdot(x_1-x_2)]}{\int d^4x_1 S(x_1,\mathbf{p_1}) \int d^4x_2 S(x_2,\mathbf{p_2})}, \qquad (2)$$

where $\mathbf{p_1}$ and $\mathbf{p_2}$ represent the momenta of the two pions, respectively, $\mathbf{K} = (\mathbf{p_1} + \mathbf{p_2})/2$, and $Q = (\mathbf{p_1} - \mathbf{p_2}, E_1 - E_2)$. Expecting that the emission function is sufficiently smooth in the momentum space, one can evaluate the correlation function by using $\mathbf{p_1}$ and $\mathbf{p_2}$ for $\mathbf{K}$ in the numerator of Eq.(2). Furthermore, the three-dimensional correlation function in $\mathbf{Q}$ is usually shown as a function of the invariant relative momentum ($Q_{\rm inv} = \sqrt{-Q^2}$) or as a function of the projection of $\mathbf{Q}$ in the "out-side-long" (*osl*) system [3, 4], defined by the beam direction ($Q_{\rm long}$), the direction along the total momentum of the two particles in the transverse plane ($Q_{\rm out}$), and the direction orthogonal to the above two directions ($Q_{\rm side}$).

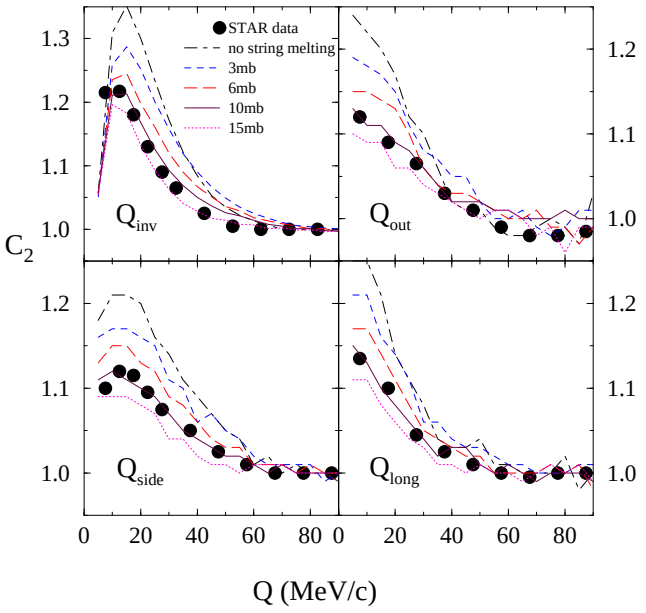

FIG. 1: Correlation functions for midrapidity charged pions with $125 < p_{\rm T} < 225$ MeV/c. Theoretical results with Coulomb corrections are shown for the default AMPT model and for the extended AMPT model with string melting and various values for σ_p. Coulomb-uncorrected correlation functions from the STAR collaboration [8] are shown by filled circles.

Using the emission function obtained from the AMPT model for central ($b = 0$ fm) Au+Au collisions at $\sqrt{s} = 130A$ GeV, we have evaluated the correlation function $C_2(\mathbf{Q}, \mathbf{K})$ in the longitudinally comoving system frame using the program Correlation After Burner [23]. In Fig. 1, we show the one-dimensional projections of the calculated correlation function including final-state Coulomb interactions for midrapidity ($-0.5 < y < 0.5$) charged pions with transverse momentum $125 < p_{\rm T} < 225$ MeV/c. Also shown are the measured π^- correlation functions from central collisions by the STAR collaboration without removing the effect due to the Coulomb interaction [8]. In evaluating the one-dimensional projections of the correlation function onto one of the $Q_{\rm out}, Q_{\rm side}$ and $Q_{\rm long}$ axes, we have integrated the other two $\mathbf{Q}$ components over the range $0 - 35$ MeV/c. The dash-dotted curves in Fig. 1 are results from the default AMPT model (no string melting) with a parton scattering cross section of $\sigma_p = 3$ mb, while other curves are those from the extended AMPT model with string melting but different values for σ_p. It is seen that with string melting both the width of the $Q_{\rm inv}$ correlation function and its height decrease with increasing σ_p. The decreasing width can be more clearly seen from the calculated correlation functions without including final-state Coulomb interactions [24], as the value of the correlation function in this case is exactly two at $Q_{\rm inv} = 0$. Since the integration of the other two $\mathbf{Q}$ components over a fixed range ($0 - 35$ MeV/c) gives a smaller value when the correlation function becomes narrower in $\mathbf{Q}$, the height of the one-dimensional projection of the correlation function decreases with increasing σ_p. To reproduce the measured one-dimensional correlation functions by the STAR collaboration, we find that a parton scattering cross section of about 10 mb is required in the extended AMPT model with string melting. Since in our model partons are converted to hadrons after they make their last scattering, the parton scattering cross section thus controls the density at which partons are converted to hadrons. A larger σ_p leads to a lower density and larger volume for the parton to hadron phase transition. We expect that the two-pion correlation data could also be reproduced by using a smaller parton scattering cross section but delaying the hadronization until the critical density is similar to the one given by the parton freezeout condition using a scattering cross section of 10 mb in the parton cascade model [24].

The size of the emission source can be determined from the emission function via the curvature of the correlation function at $\mathbf{Q} = 0$:

$$R_{ij}(K)^2 = -\frac{1}{2}\frac{\partial^2 C_2(\mathbf{Q},\mathbf{K})}{\partial Q_i \partial Q_j}\bigg|_{\mathbf{Q}=0}$$
$$= D_{x_i,x_j}(K) - D_{x_i,\beta_j t}(K) - D_{\beta_i t,x_j}(K) + D_{\beta_i t,\beta_j t}(K), \quad (3)$$

where $x_i (i = 1-3)$ denotes the projections of the particle position at freezeout in the *osl* system, i.e., $x_{\rm out}$, $x_{\rm side}$ and $x_{\rm long}$, and $\beta = \mathbf{K}/K_0$ with K_0 being the average energy of the two particles. In the second line of Eq.(3), we have the variance $D_{x,y} = \langle x \cdot y \rangle - \langle x \rangle \langle y \rangle$, with $\langle x \rangle$ denoting the average value of x.

Since only the correlation function is measured in experiments, the size of emission source is usually estimated by fitting the measured correlation function $C_2(\mathbf{Q}, \mathbf{K})$, that has been corrected for effects due to final-state Coulomb interactions, with a four-parameter Gaussian function:

$$C_2(\mathbf{Q}, \mathbf{K}) = 1 + \lambda \exp\left(-\sum_{i=1}^{3} R_{ii}^2(K) Q_i^2\right). \quad (4)$$

If the emission source is Gaussian in space-time, then for central heavy ion collisions considered here the radius parameters obtained from the above Gaussian fit to the correlation function would be the same as those determined directly from the emission function of the source via Eq.(3). However, because of space-time correlations in the emission function, such as those induced by the collective flow, the radius parameters in general do not give the true source size.

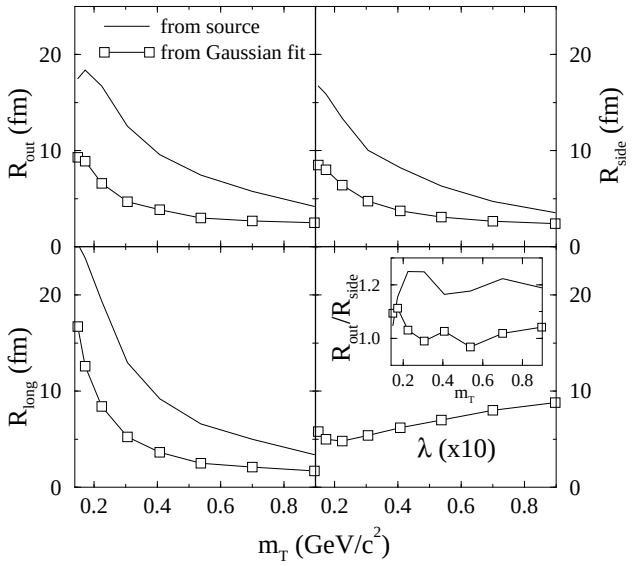

FIG. 2: Source radii from the emission function (solid curves) as well as the fitted radius and λ parameters from the Gaussian fit to the correlation function (curves with squares) for midrapidity pions as functions of pion transverse mass $m_{\rm T}$. The inset shows the corresponding ratio $R_{\rm out}/R_{\rm side}$.

In Fig. 2, we show by solid curves the transverse mass ($m_{\rm T}$) dependence of the source radii $R_{\rm out}$ (upper-left panel), $R_{\rm side}$ (upper-right panel), and $R_{\rm long}$ (lower-left panel) determined from the emission function for midrapidity charged pions given by the AMPT model with string melting and parton cross section of $\sigma_p = 10$ mb for central Au+Au collisions at $\sqrt{s} = 130A$ GeV. The radius parameters determined from the Gaussian fit to the three-dimensional correlation function in $\mathbf{Q}$ without including final-state Coulomb interactions are shown by curves with squares. For the $m_{\rm T}$ values shown here, these radius parameters are about a factor of 2 to 3 smaller than the source radii obtained directly from the emission function. The emission source from the AMPT model thus deviates appreciably from a Gaussian one. The radius parameters from the Gaussian fit to the correlation function have similar values as the experimental ones from a Gaussian fit to the measured correlation function after correcting for the final-state Coulomb interactions [8]. The parameter λ (scaled up by a factor of 10) from the Gaussian fit to the correlation function is shown in the lower-right panel by the curve with squares. It has a value of about 0.5 at low $m_{\rm T}$ but increases to about 1 at large $m_{\rm T}$. Both the source radii and fitted radius parameters decrease with increasing $m_{\rm T}$. On the other hand, these radii increase with increasing parton scattering cross section as a result of both a larger source size and stronger collective expansion [24].

Since Eq.(3) gives

$$R^2_{\rm out} = D_{x_{\rm out},x_{\rm out}} - 2\, D_{x_{\rm out},\beta_\perp t} + D_{\beta_\perp t,\beta_\perp t}, \quad (5)$$

and $R^2_{\rm side} = D_{x_{\rm side},x_{\rm side}}$, the ratio $R_{\rm out}/R_{\rm side}$ contains information about the duration of emission and has been studied extensively [6, 8]. This connection between $R_{\rm out}$ and the emission duration becomes clearer if we neglect the $x_{\rm out} - t$ correlation term $D_{x_{\rm out},\beta_\perp t}$ in Eq.(5). In the inset of the lower-right panel of Fig. 2, we show the ratio $R_{\rm out}/R_{\rm side}$ for midrapidity charged pions. It is seen that the ratio $R_{\rm out}/R_{\rm side}$ obtained from the emission function (solid curve) has a value between 1.0 and 1.3 as in predictions based on the hydrodynamical model with freezeout treated via the hadronic transport model [6]. However, with the radius parameters extracted from the Gaussian fit to the correlation function, the ratio $R_{\rm out}/R_{\rm side}$ becomes much closer to 1, similar to the experimental values extracted from the measured correlation function [8].

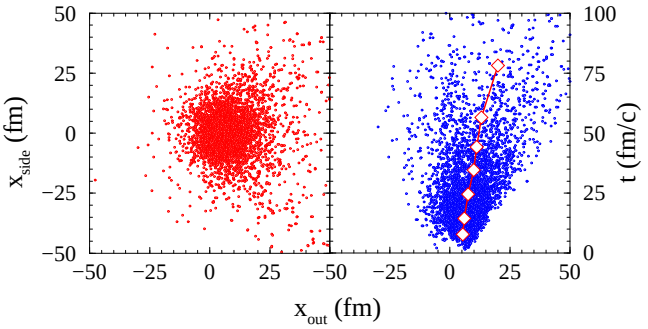

FIG. 3: $x_{\rm out} - x_{\rm side}$ (left panel) and $x_{\rm out} - t$ (right panel) distributions at freezeout for midrapidity charged pions with $125 < p_{\rm T} < 225$ MeV/c. The curve with open diamonds represents $\langle x_{\rm out}\rangle$ as a function of t.

To investigate the reason for the large difference between the source radii obtained directly from the emission function and from the Gaussian fit to the correlation function, we show in Fig. 3 the $x_{\rm out} - x_{\rm side}$ distribution (left panel) and the $x_{\rm out} - t$ distribution (right panel) at freezeout for midrapidity pions with $125 < p_{\rm T} < 225$ MeV/c from the AMPT model with string melting and $\sigma_p = 10$ mb. It is seen that the emission source is shifted in the direction of the pion transverse momentum, i.e, $\langle x_{\rm out}\rangle > 0$. This positive shift in $x_{\rm out}$ results from the collective expansion of the emission source [14].

If the width in $x_{\rm out}$ were much smaller than the average value $\langle x_{\rm out}\rangle$, the emission source would have a shell-like

shape, similar to the emission source with strong opacity in the hydrodynamical model [11]. The emission source also shows a large halo around a central core. The halo consists not only of pions from decays of long-lived resonances such as the ω but also of thermal pions. In calculating the correlation function, we have included pions from the decay of η resonances as in experiments. Their effects on the radius parameters obtained from the Gaussian fit to the correlation function are thus included. On the other hand, we have excluded these pions in evaluating the source radii from the emission function due to the long lifetime of η. Since long-lived resonances mainly affect the correlation function at small relative momenta [25], they are important in determining the λ parameter.

As to the $x_{\rm out} - t$ distribution of the emission function shown in the right panel of Fig. 3, it has a strong positive $x_{\rm out} - t$ correlation as clearly seen from the solid curve with open diamonds, which shows that the average value $\langle x_{\rm out}\rangle$ increases with the freezeout time t. The $x_{\rm out} - t$ correlation leads to a large positive value for the $x_{\rm out} - t$ correlation term $D_{x_{\rm out},\beta_\perp t}$ in Eq.(5). For pions included in generating Fig. 3, the value of $D_{x_{\rm out},\beta_\perp t}$ is 168 fm^2 and is appreciable compared to 185 and 431 fm^2, respectively, for the first and last terms in Eq.(5). This makes it difficult to extract information about the duration of emission from the ratio $R_{\rm out}/R_{\rm side}$. Similar results have been seen previously in studies based on the RQMD model at SPS [26, 27]. We note that the imaging method [28], developed for extracting the emission function of a source from the correlation function, will be very useful for verifying the non-Gaussian features of the emission source in high energy heavy ion collisions.

In summary, we have studied the pion interferometry in relativistic heavy ion collisions at RHIC. Using a multiphase transport model that includes both initial partonic and final hadronic interactions, we find that the two-pion correlation function is sensitive to the parton scattering cross section, which controls the density at which the parton-to-hadron transition occurs in the AMPT transport model. To reproduce the measured correlation function in central Au+Au collisions at $\sqrt{s} = 130A$ GeV requires both the melting of initial strings to partons and a large parton scattering cross section, i.e., a low parton density for the transition from the partonic to the hadronic matter. We further find that the emission source is non-Gaussian in space and time. It not only shifts significantly to the direction along the pion transverse momentum but also has a strong correlation between this displacement and the freezeout time. Consequently, the source radii extracted directly from the emission function are about a factor of 2 to 3 larger than the radius parameters extracted from a Gaussian fit to the three-dimensional correlation function. Furthermore, the ratio $R_{\rm out}/R_{\rm side}$ obtained from the emission function is larger than that extracted from a Gaussian fit to the correlation function, which is found to be close to one. Although the correlation function requires only the space-time information of pions at freezeout, it is shown to be sensitive to the partonic dynamics during the early stage of heavy ion collisions. The study of pion interferometry thus helps to confirm the formation of the partonic matter at RHIC and to study its properties.

We appreciate useful discussions with L.-W. Chen, P. Danielewicz, M. Gyulassy, U. Heinz, M. Lisa, M. Murray, P. Philip, T. Csörgö, S. Pratt, N. Xu, and Q.H. Zhang. This paper is based on work supported by the U.S. National Science Foundation under Grant Nos. PHY-9870038 and PHY-0098805, the Welch Foundation under Grant No. A-1358, and the Texas Advanced Research Program under Grant No. FY99-010366-0081.

[1] R. Hanbury Brown and R.Q. Twiss, Nature (London) **178**, 1046 (1956).
[2] S. Pratt, Phys. Rev. Lett. **53**, 1219 (1984).
[3] G. Bertsch *et al.*, Phys. Rev. C **37**, 1896 (1988).
[4] S. Pratt *et al.*, Phys. Rev. C **42**, 2646 (1990).
[5] D. H. Rischke and M. Gyulassy, Nucl. Phys. A **608**, 479 (1996).
[6] S. Soff *et al.*, Phys. Rev. Lett. **86**, 3981 (2001).
[7] S. Soff *et al.*, Phys. Rev. Lett. **88**, 072301 (2002); J. Phys. G **28**, 1885 (2002).
[8] C. Adler *et al.*, STAR Collaboration, Phys. Rev. Lett. **87**, 082301 (2001).
[9] S. C. Johnson, PHENIX Collaboration, Nucl. Phys. A **698**, 603 (2002).
[10] K. Adcox *et al.* [PHENIX Collaboration], Phys. Rev. Lett. **88**, 192302 (2002).
[11] B. Tomasik and U. W. Heinz, nucl-th/9805016.
[12] B. Zhang *et al.*, Phys. Rev. C **61**, 067901 (2000).
[13] Z. W. Lin *et al.*, Phys. Rev. C **64**, 011902 (2001); Nucl. Phys. A **698**, 375 (2002).
[14] Z. W. Lin and C. M. Ko, Phys. Rev. C **65**, 034904 (2002).
[15] X. N. Wang and M. Gyulassy, Phys. Rev. D **44**, 3501 (1991).
[16] B. Zhang, Comput. Phys. Commun. **109**, 193 (1998) .
[17] T. Sjostrand, Comput. Phys. Commun. **82**, 74 (1994).
[18] B. A. Li and C. M. Ko, Phys. Rev. C **52**, 2037 (1995) .
[19] D. Kharzeev and M. Nardi, Phys. Lett. B **507**, 121 (2001).
[20] B. Zhang *et al.*, Phys. Rev. C **62**, 054905 (2000).
[21] K. H. Ackermann *et al.*, STAR Collaboration, Phys. Rev. Lett. **86**, 402 (2001).
[22] U. A. Wiedemann and U. W. Heinz, Phys. Rept. **319**, 145 (1999) .
[23] S. Pratt *et al.*, Nucl. Phys. A **566**, 103c (1994).
[24] Z. W. Lin *et al.*, in preparation.
[25] T. Csörgö *et al.*, Z. Phys. C **71**, 491 (1996) .
[26] J. P. Sullivan *et al.*, Phys. Rev. Lett. **70**, 3000 (1993).
[27] D. E. Fields *et al.*, Phys. Rev. C **52**, 986 (1995).
[28] D. A. Brown and P. Danielewicz, Phys. Lett. B **398**, 252 (1997); Phys. Rev. C **57**, 2474 (1998); *ibid* **64**, 014902 (2001); S. Y. Panitkin and D. A. Brown, Phys. Rev. C **61**, 021901 (2000).